The M33 Synoptic Stellar Survey. III. Miras and LPVs in griJHK*S*

Tarini et al. 2024, MNRAS, 000, 1–12

Reporter: Yu Pan

2024/10/28

OUTLINE

Introduction

The importance of studying Miras

- Miras can serve as one of these primary distance indicators.
- Miras are Asymptotic Giant Branch (AGB) stars that can pulsate in fundamental or overtone modes with typical periods ranging from ~100 to ~3,000 days.
- Mira variability is cyclic, characterized by large peak-to-trough amplitudes at optical wavelengths ($\Delta I > 0.8$ mag), and long-term variations in mean magnitude. Miras also vary in the near-infrared (NIR) with smaller amplitudes ($\Delta K_S > 0.4$ mag).
- Given their low- to intermediate-mass progenitors ($0.8M_\odot < M < 8M_\odot$), they are common and can be found across all types of galaxies.

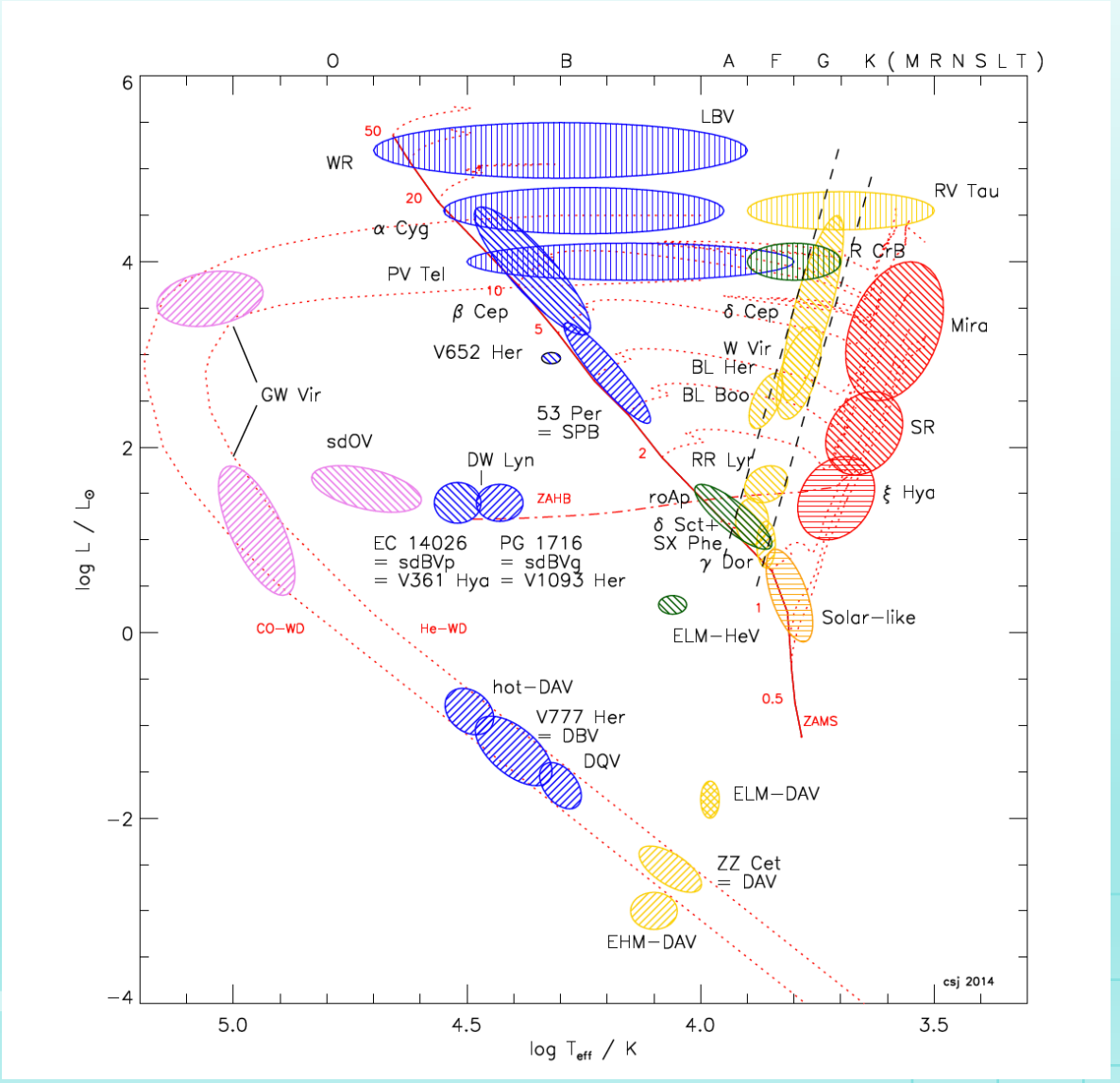

Introduction

Mira's PLR

- Miras follow tight NIR Period-Luminosity relations (PLRs). In the Large Magellanic Cloud (LMC), O-rich Miras have K-band PLRs with low scatter (σ = 0 .12 mag) that is comparable to the scatter of Cepheid PLRs in the same band (σ = 0.09 mag).
- O-rich Miras with $P < 400$ d have been demonstrated to be useful as extragalactic distance indicators. Yuan et al. (2017a) used I-band observations from Macri et al. (2001) and Pellerin & Macri (2011) to identify 1,847 Mira candidates in M33. Their study was extended in Yuan et al. (2018) with sparsely-sampled JHK_S light curves, where they obtained NIR PLRs for O-rich Miras and a distance modulus of 24.80 ± 0.06 mag for M33.

OBSERVATIONS AND DATA REDUCTION

MegaCam and WIRCam Observations

They used archival pipeline-processed optical observations of M33 taken with the MegaCam instrument on the CFHT.

MegaCam is a wide-field (1 deg. on a side) optical imager consisting of 36 CCDs with a plate scale of 0.″187 per pixel. This yielded a typical coverage of 29, 27, 28 and 1 nights in $griz$, respectively.

They also used archival pipeline-processed NIR observations of M33 obtained with the WIRCam on CFHT.

WIRCam consists of four detectors with a combined field of view 20.′5 on a side and a plate scale of 0.″3 per pixel. This yielded an average of 9, 6 and 3 epochs in JHKS, respectively, for locations imaged in a given band.

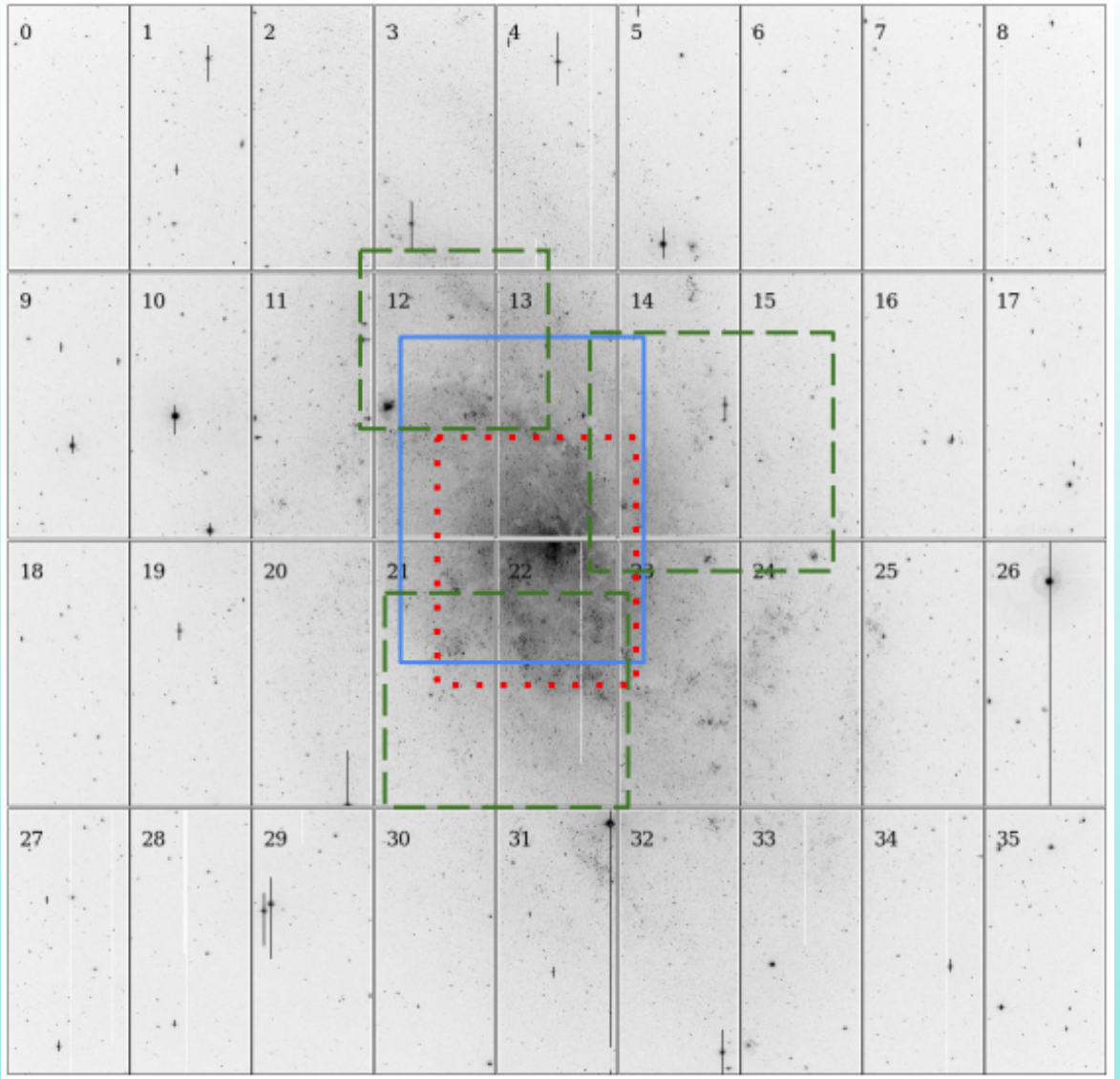

Figure 1. Mosaic of a typical CFHT MegaCam image of M33 with the CCD numbers marked, also showing the areas covered by WIRCam in J (blue, solid), H (green, dashed), and KS (red, dotted) fields. North is up and east is to the left.

OBSERVATIONS AND DATA REDUCTION

Crowding corrections

- Biased magnitude measurements have long been recognized as an issue affecting crowded-field photometry of faint stars.
- The standard approach to characterizing and correcting this bias relies on the injection of artificial stars in the vicinity of, and with the same flux as, the objects of interest.
- They carried out the same photometric procedures on each of the artificial images as previously done in the real ones, identified the artificial sources and compared the recovered and input magnitudes.
- Crowding corrections are minimal for objects with m <19: 0.014 ± 0.054 (J), 0.009 ± 0.067 (H), -0.002 ± 0.042 (KS). ~ 22% of the variables had crowding corrections exceeding 0.1 mag or uncertainties in those corrections beyond 0.1 mag; they were flagged accordingly and excluded from the final samples.

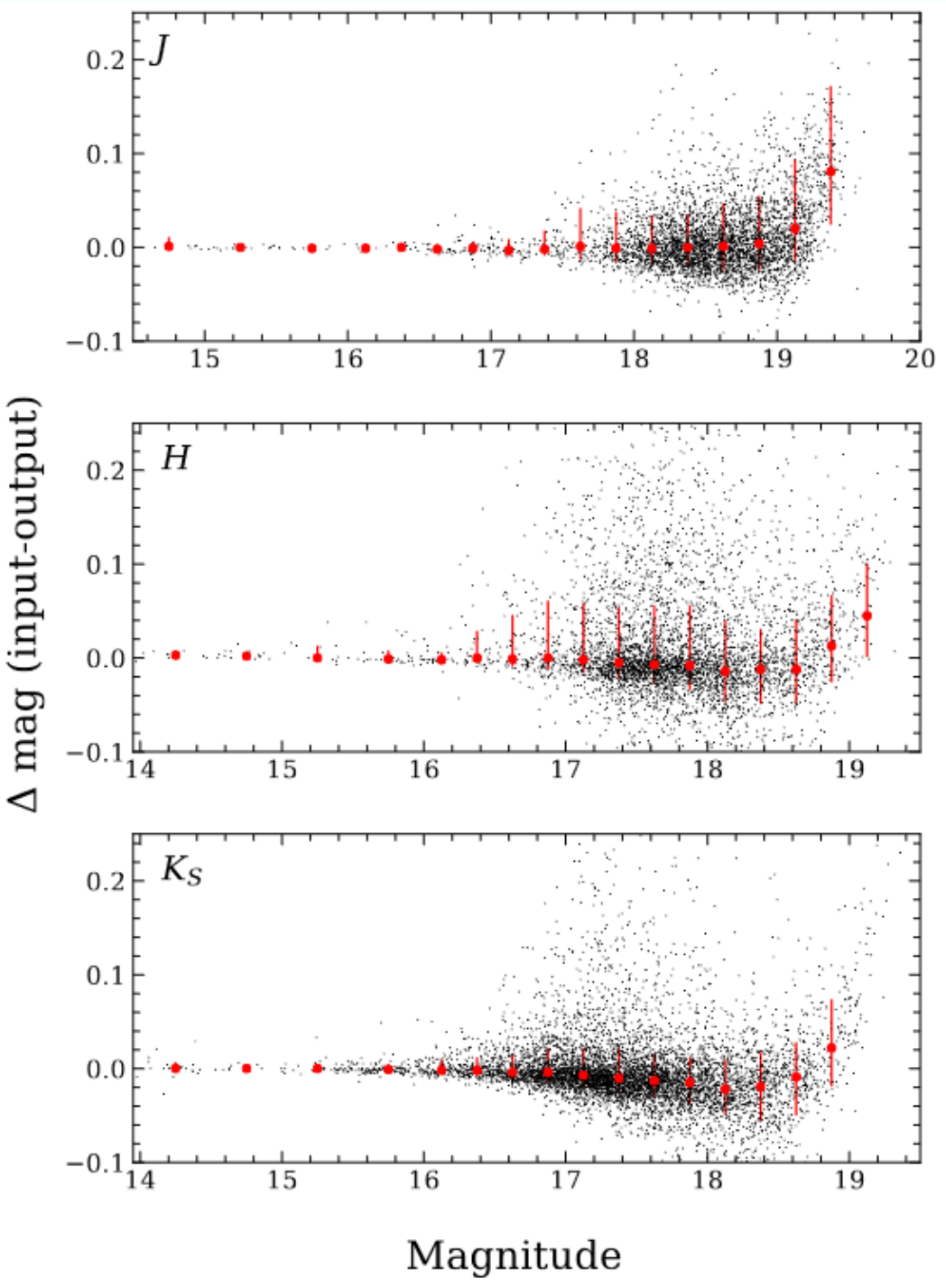

IDENTIFYING LPVS AND MIRA CANDIDATES USING OPTICAL AND NIR OBSERVATIONS

They identified ~1.15 million unique objects from photometry which had at least one detection in one of the *gri* bands.

Left: Hess diagrams in the optical bands. Individual stars are plotted where the source density drops below 200 objects per bin. Recovered Miras from Yuan et al. (2017a) are shown using red points. Mira recovery varies across filters. Not all recovered Miras were kept in our final samples, due to quality cuts.

Right: Hess diagrams in the NIR bands.

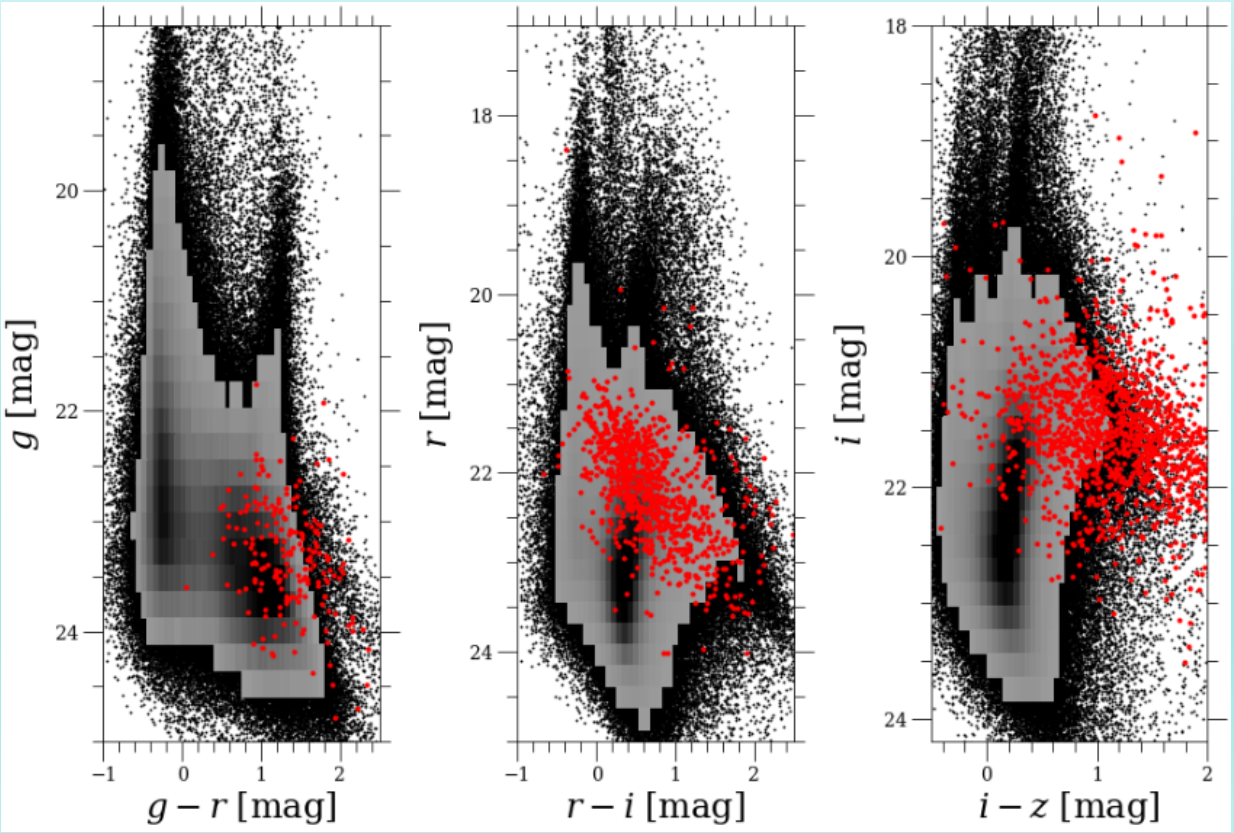

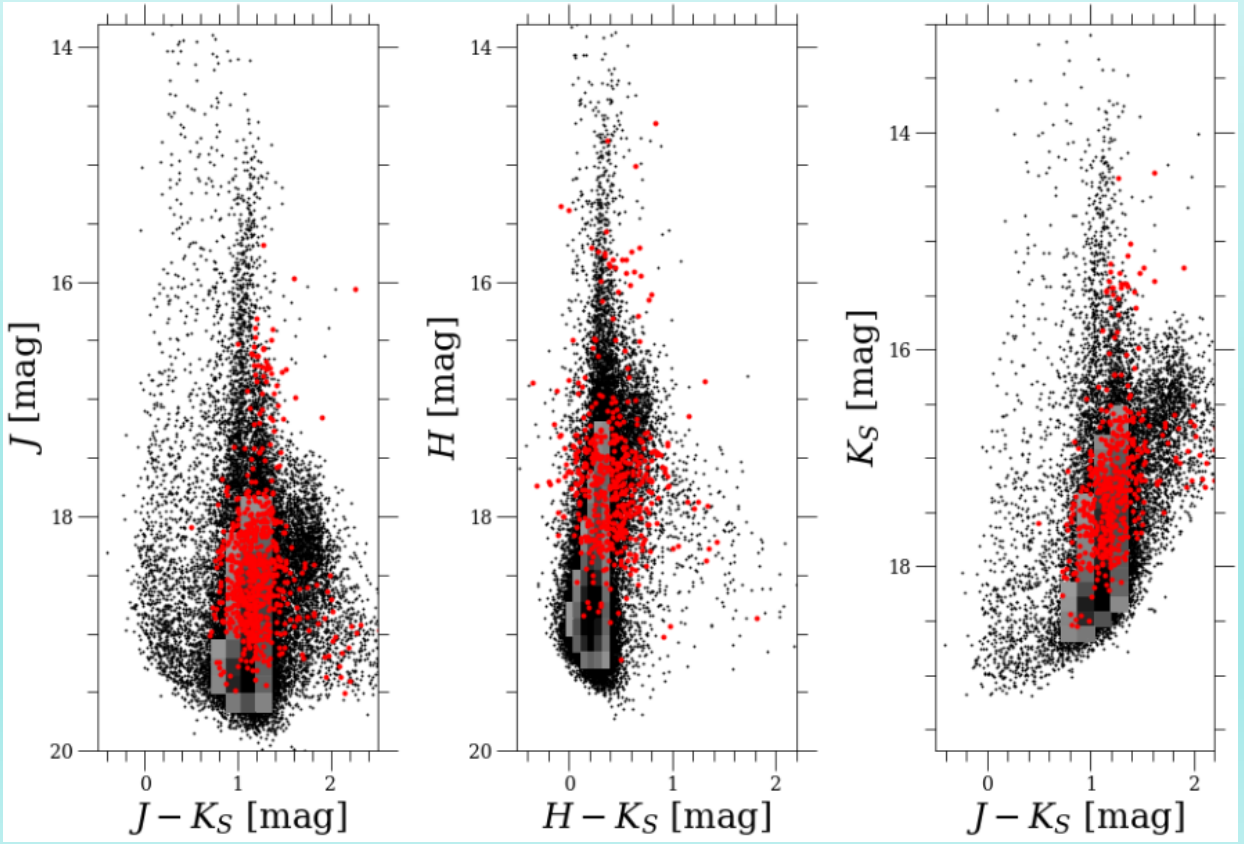

IDENTIFYING LPVS AND MIRA CANDIDATES USING OPTICAL AND NIR OBSERVATIONS

3.1. Initial selection

- They began the selection of LPVs and Mira candidates by making variability, color, and amplitude cuts based on the optical data.
- They were left with 14,312 variables, which included 1,342 of the Miras identified in Yuan et al. (2017a).

Table A3. Selection of LPVs and Mira candidates.

Criterion	N
1. Detected in $\geq$1 of gri	1,158,951
2. Detected in i	1,036,491
3. $J_i \geq 0.75$	69,798
4. $r-i \geq 0$ or no r	65,609
5. $R_i \geq 0.3$ mag	39,660
6. Detected in $\geq$1 of JHK_S	14,312

IDENTIFYING LPVS AND MIRA CANDIDATES USING OPTICAL AND NIR OBSERVATIONS

3.2. Light curve fits

- They fit the available griJHK*S* light curves of these variables using a simple sinusoidal model, defined for a given band as

$$m(t_i) = \overline{m} - A\sin(2\pi t_i/P + \phi)$$

where m is the magnitude at time ti, m is the mean magnitude, A is the semi-amplitude, P is the period, and ϕ is a phase offset.

- They fit each variable using 55 trial periods equally spaced every 0.02 log P, spanning $1.925 \leq \log P \leq 3.005$, and selected the fit with the lowest χ_ν^2.
- They found good agreement (defined as $\Delta P < 50$ d) for ~78.1% of the objects, with most of the others lying along the ±1/365 d alias relations.

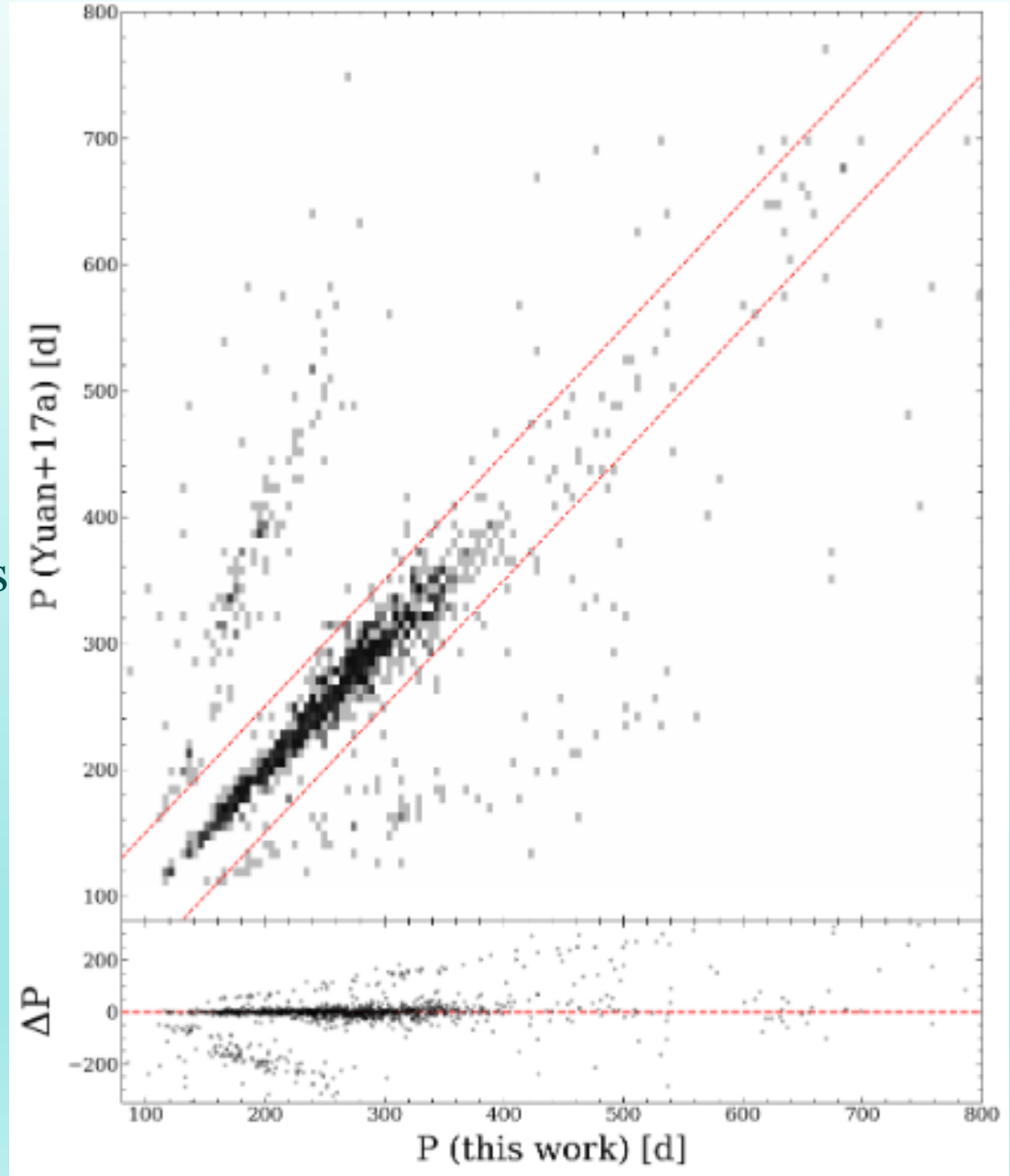

IDENTIFYING LPVS AND MIRA CANDIDATES USING OPTICAL AND NIR OBSERVATIONS

3.2. Light curve fits

- They fit the coupled sinusoidal model to all 14,312 variables to derive *P* and other properties for each object.
- Fig shows the light curves and best-fit model for a recovered Mira
- Table presents the properties and associated uncertainties of all 14,312 LPVs

ID	RA	Dec	*P*	*i*	*J*	*H*	K_S	*r*	*g*	A_i	A_J	A_r	A_g
	[deg]		[d]			[mag]					[mag]		
01322479+3047175	23.103285	30.788191	389.05	20.348	...	18.074	...	21.936	23.175	0.766	0.105	0.316	0.326
01322533+3036126	23.105537	30.603506	1071.52	21.644	...	17.339	...	22.958	...	0.194	0.204	0.266	...
01322583+3047503	23.107637	30.797293	1071.52	20.501	...	18.077	...	22.071	23.478	0.935	0.142	0.452	0.508
01322793+3039553	23.116392	30.665359	117.82	21.206	...	17.756	...	23.215	...	0.155	0.092	0.257	...
01322879+3049434	23.119947	30.828728	365.78	21.066	...	17.036	...	22.939	...	0.813	0.125	0.453	...
01323222+3041360	23.134270	30.693346	361.46	21.477	...	17.590	...	22.586	...	0.568	0.215	0.777	...
01323651+3037358	23.152111	30.626614	161.01	21.957	...	17.388	...	...	...	0.305	0.027	...	...
01330333+3038314	23.263865	30.642057	244.74	21.063	20.012	18.492	...	21.836	...	0.144	0.082	0.152	...
01330346+3041361	23.264431	30.693350	408.17	20.696	17.825	16.674	...	21.723	...	0.752	0.498	0.904	...
01330349+3042025	23.264532	30.700701	411.09	20.863	18.972	18.044	...	...	23.124	0.358	0.411	...	1.056
01330365+3030497	23.265224	30.513803	395.22	20.232	18.986	...	...	20.722	22.154	0.365	0.248	0.494	0.219
01330549+3038194	23.272890	30.638735	289.39	21.574	18.099	17.620	...	...	...	1.061	0.245	...	...
01330596+3037390	23.274841	30.627512	144.20	21.362	19.027	18.253	...	22.372	...	0.311	0.307	0.673	...
01330678+3033068	23.278263	30.551893	448.70	21.978	19.184	...	17.483	...	...	0.263	0.178	...	...
01330706+3034548	23.279436	30.581900	297.75	22.608	18.632	...	17.336	...	...	2.445	0.376	...	...
01330740+3032356	23.280830	30.543226	410.86	23.253	...	...	18.810	...	...	0.520	0.118	...	...
01330771+3043034	23.282106	30.717609	188.02	21.211	19.661	...	16.971	22.374	...	0.352	0.248	0.493	...
01330991+3035253	23.291283	30.590351	95.80	22.131	19.200	...	17.895	...	...	0.245	0.073	...	...

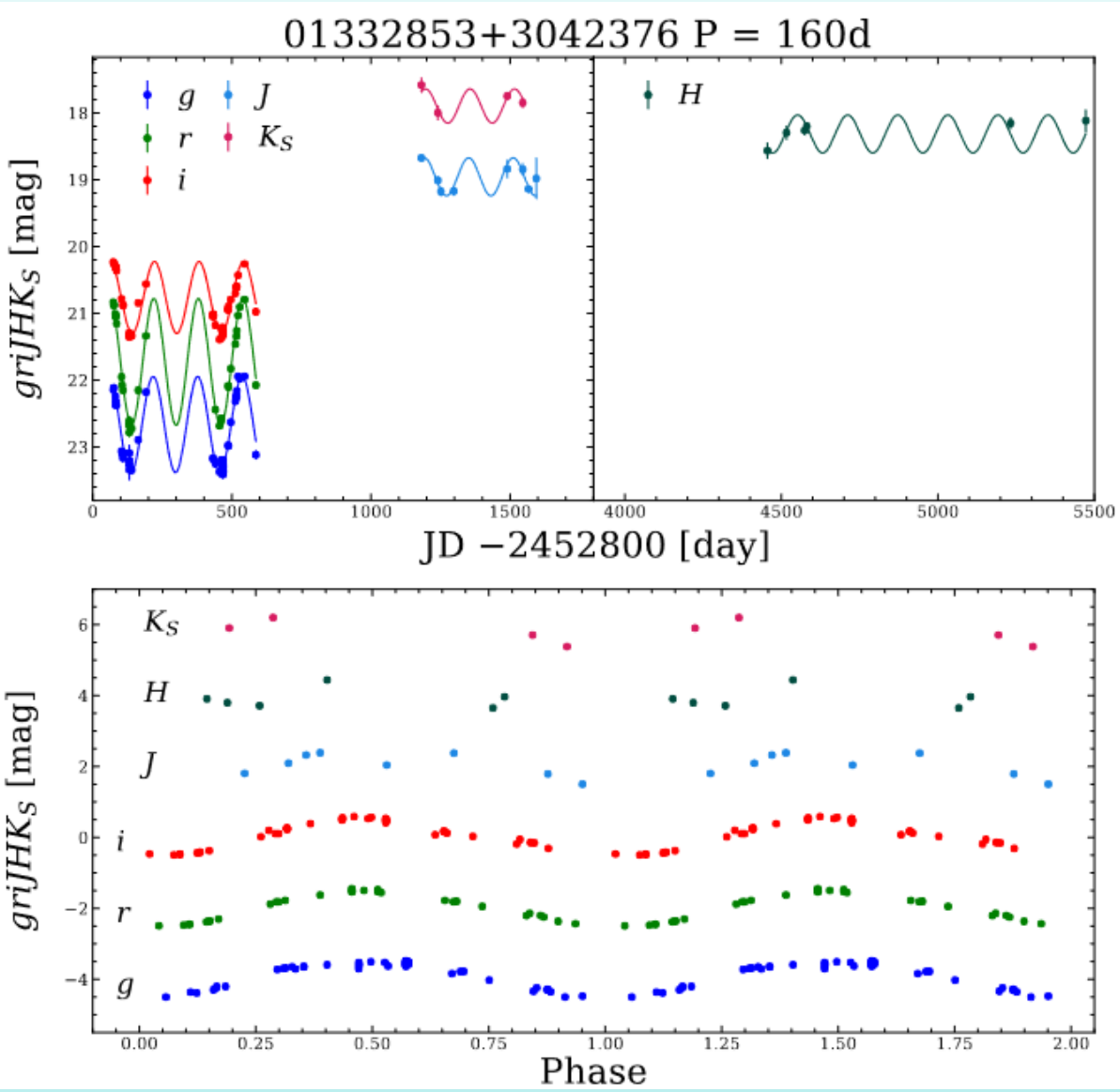

IDENTIFYING NEW MIRA CANDIDATES

- They applied several quality cuts to the 12,970 LPVs not previously classified as Miras.

(i) 2,891 with crowding corrections or uncertainties in these corrections exceeding 0.1 mag;
(ii) 1,336 with best-fit periods near the lower or upper limits of our grid search;
(iii) 296 with abnormally blue colors
(iv) 2,303 faint variables lying below the first-overtone and fundamental mode groups.

- Resulted in a classification sample of 6,144 variables. These cuts were also applied to the recovered Miras from Yuan et al. (2018); 934 were selected for further analysis.

IDENTIFYING NEW MIRA CANDIDATES

Machine Learning Classification

- They used six machine learning methods as classifiers to identify new Mira candidates.
- They trained and validated the classifiers using the Mira candidates(934) from Yuan et al. (2018) that we recovered in our data.
- They fit Period-Luminosity relations to various subsets of the 3,052 newly-classified and visually-inspected Mira candidates and the 934 Miras from yuan et al.(2018).

Classifier	Passed	Visual
Logistic Regression	2,335	2,206
Random Forest	2,533	2,404
Linear Discriminant Analysis	2,800	2,637
Quadratic Discriminant Analysis	2,388	2,271
Kernel SVM	2,077	1,989
Bagging SVM	2,511	2,384
Any 1 classifier	3,251	3,052
At least 3 classifiers	2,595	2,454
All 6 classifiers	1,746	1,686

IDENTIFYING LPVS AND MIRA CANDIDATES USING OPTICAL AND NIR OBSERVATIONS

Classification into fundamental and first overtone pulsation mode subtypes

Figs show the resulting period-magnitude and period-Wesenheit diagrams. Two obvious sequences can be seen in all the NIR relations.These correspond to first-overtone (FO) and fundamental-mode (FU) pulsators. In this way, 3,986 variables were classified as either first overtone or fundamental mode.

$$W_{JK_S} = K_S - R^K_{JK_S}(J - K_S); \quad W_{JH} = H - R^H_{JH}(J - H)$$

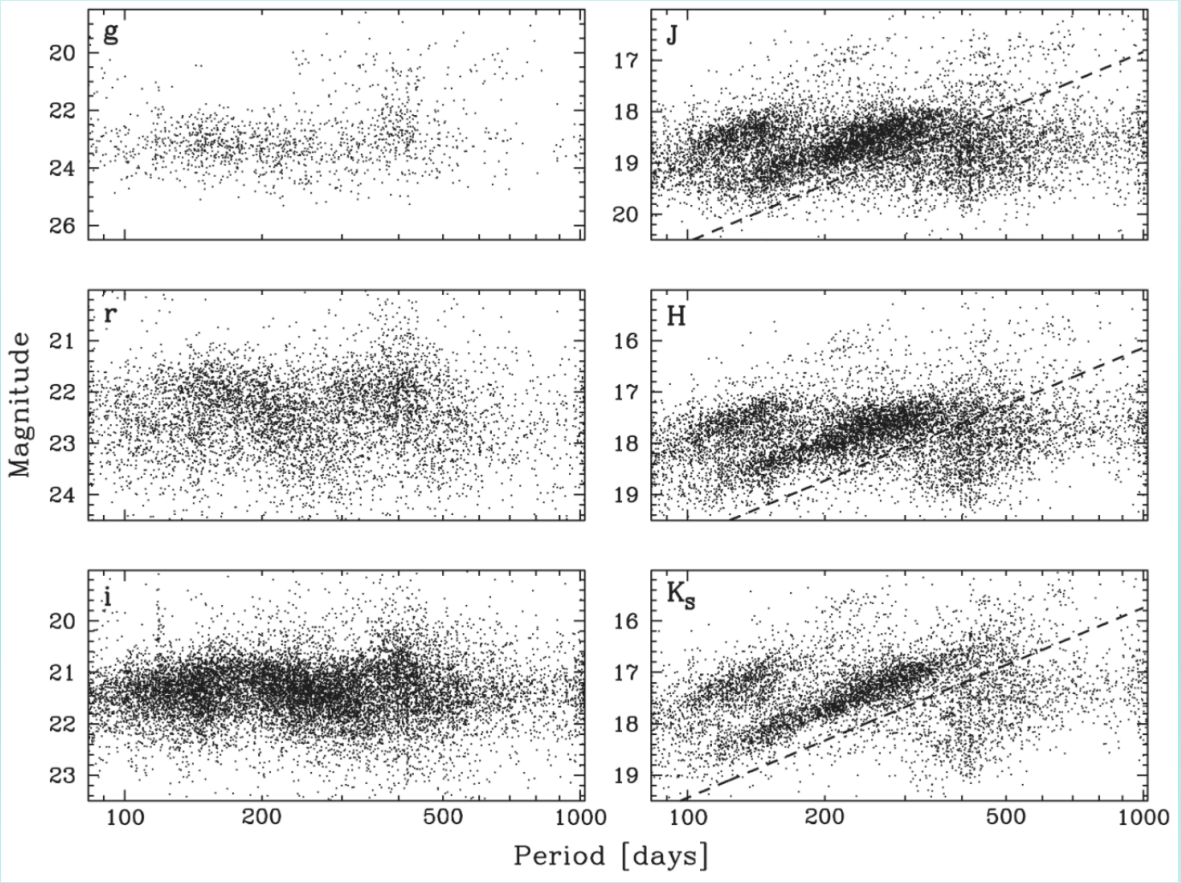

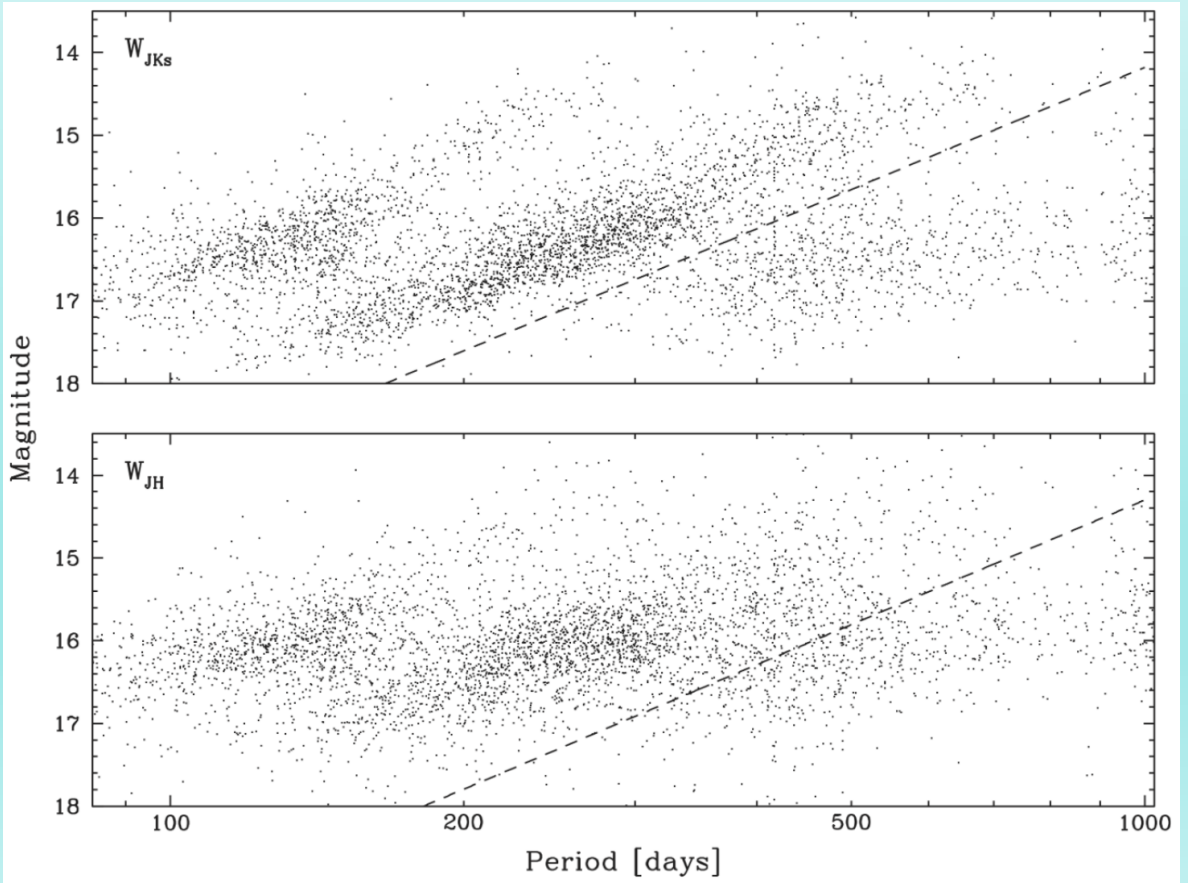

IDENTIFYING LPVS AND MIRA CANDIDATES USING OPTICAL AND NIR OBSERVATIONS

Classification into O- and C-rich subtypes

- The LMC is an ideal system to derive photometric-based classification methods for Miras given the better quality light curves that can be obtained for its variables.
- Soszyński et al. (2009) show that Miras can be reliably separated into O- and C-rich types in the $V - I$ vs. $J - KS$ plane.
- Yuan et al. (2018) also showed that O- and C-rich Miras can be separated well in the $J - H$ vs. $H - KS$ plane.
- 2,709 were classified as either O- or C-rich.

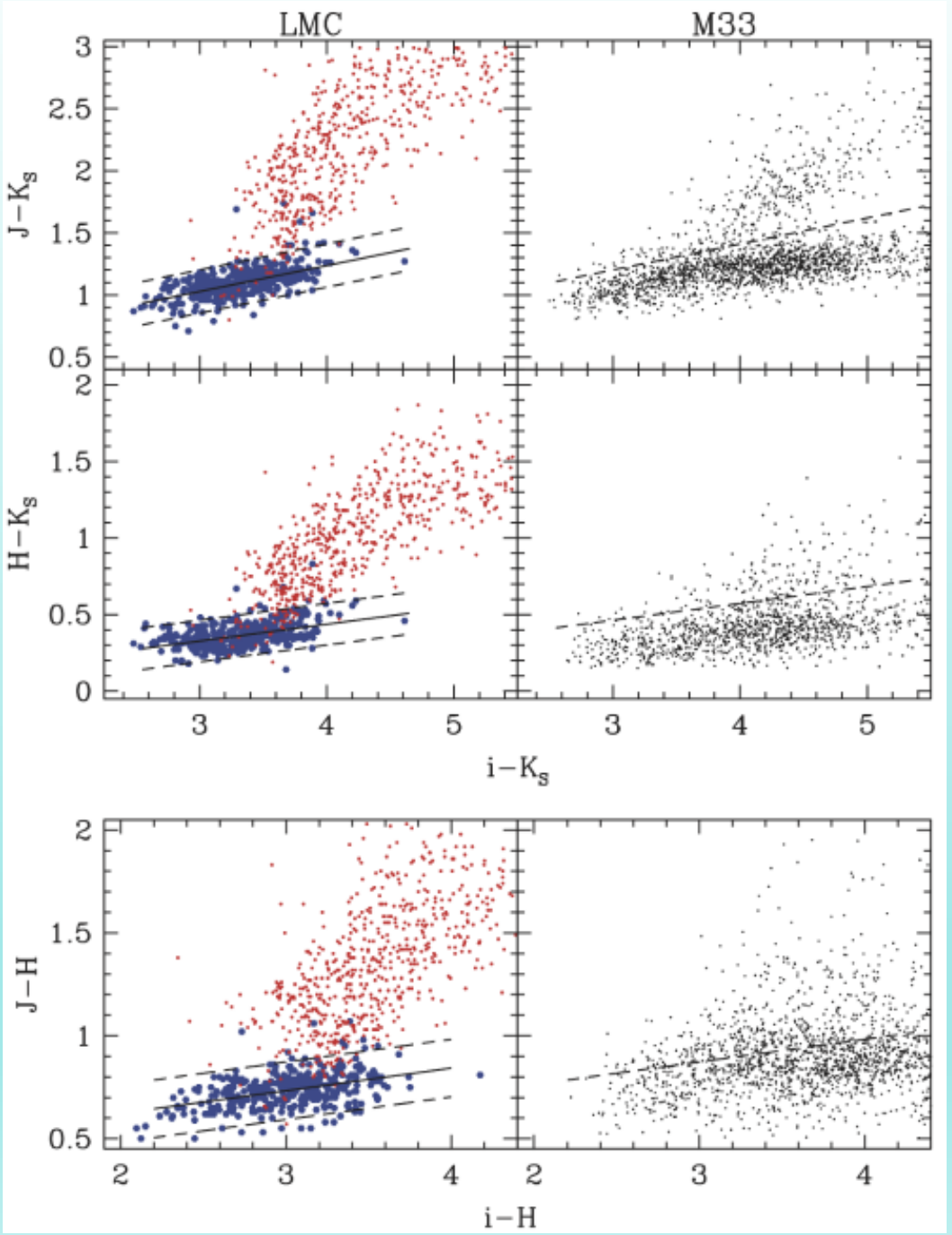

Left: Color-color relations of OGLE-III Miras in the LMC. Blue and red symbols indicate O- and C-rich variables, respectively. The solid lines are the best-fit linear relations of O-rich objects, with dashed lines indicating the $\pm 2\sigma$ dispersion.
Right: Same relations for our final M33 samples (**2709**), with dashed lines indicating the division between O- and C-rich variables.

IDENTIFYING NEW MIRA CANDIDATES

Comparison with other work

- They compared the mean magnitudes for Miras in common between our sample and theirs and found good agreement.
- They estimate a Mira-based distance to M33 using the $WJKS$ PLRs for fundamental-mode O-rich Miras with $P < 400$ d.
- They obtain $\mu M33 = 24.629 \pm 0.046$ mag, in good agreement with previous determinations based on a variety of distance indicators (see Breuval et al. 2023)

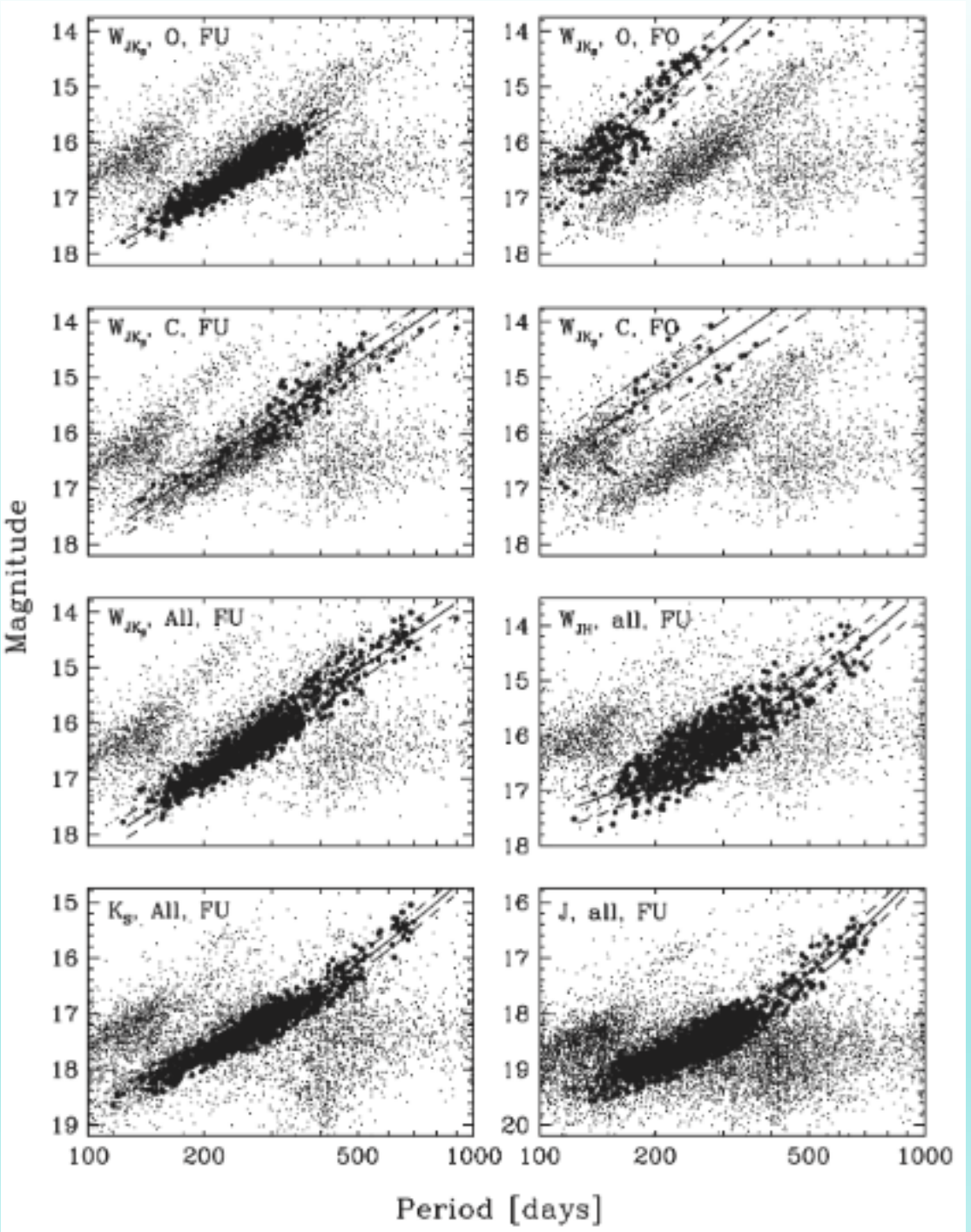

Conclusion

- We used multiband observations to identify over 13,000 new Mira candidates and LPVs in M33.
- We showed that Mira candidates can be robustly identified by using optical light curves and machine learning techniques, and our measurements in SDSS bands can be used to guide Mira searches in the Rubin/LSST era. We use near-infrared measurements to further confirm Mira candidates and classify them into various subsamples, detecting for the first time a clear first-overtone pulsation sequence in this galaxy.
- We also show that NIR observations are very relevant to creating high fidelity samples of Miras for distance measurements. We use O-rich fundamental-mode Miras with $P < 400$ d to determine a distance modulus for M33 of $\mu = 24.629 \pm 0.046$ mag.

THANKS!